iScience, Volume *24*

Supplemental information

Macrophage recruitment in immune-privileged lens during capsule repair, necrotic fiber removal, and fibrosis

Yuting Li, Zhen Li, Yumeng Quan, Hongyun Cheng, Manuel A. Riquelme, Xiao-Dong Li, Sumin Gu, and Jean X. Jiang

Figure S1. Deletion of both Cx50 and AQP0 in dKO attenuated lens growth and increased extracellular spaces, Related to STAR Methods. (A) Weight and **(B)** diameter of lenses of WT, Cx50 KO, AQP0 KO and dKO mice at various ages. **(C)** The ratio of lens weight to volume. **(D)** H&E images of dKO lens at various ages (n=3) and the percentages of empty extracellular spaces to entire lens areas in dKO lens.

Figure S2. Disorganization of lens structures and gradual disappearance of "tail-like" tissue at lens posterior during lens development of dKO mice, Related to STAR Methods. (A) Images of H&E stained midsagittal paraffin tissue sections of lenses from WT (upper panel) and dKO (lower panel) mice at various development periods. Scale bar = 500 μm. **(B)** A diagram illustrating higher resolution images of different lens regions (indicated by frames) of WT and dKO at various development periods; **(C)** epithelium and anterior region; **(D)** equator region; **(E)** central region, and **(F)** posterior region. Empty extracellular space (asterisks), disorganized central nuclei (black arrowheads), liquefaction necrosis (black arrows), and macrophages (empty black arrows). Scale bar = 50 μm in **C**-**F**.

Figure S3. Increased apoptotic lens fibers in dKO, Related to STAR Methods. (**A**) A diagram illustrating higher resolution cryosection images of different lens regions of WT and dKO (indicated by frames) at P15 and P30. (**B**-**D**) Fluorescence images of co-immunostaining with anti-CD68 (red), anti-caspase-3 (Casp-3, purple) and Cx46 antibody (Cx46, green) at equator region **(B)**, central region (**C**), and the "tail-like" region (**D**). Scale bar = 50 μm.

Figure S4. Thickness of anterior capsule, Related to Figure 4E. The thickness of anterior capsule in WT and dKO lenses (n=3) at P15, P60 and 1 year. **, $P < 0.01$; ****, $P < 0.0001$.

Figure S5. TGF-β, VEGF-α and GAL-3 are involved in capsule sealing by fibrosis, Related to STAR Methods. The mRNA expression of **(A)** TGFb1, **(B)** VEGFA and **(C)** LGALS3 in WT (n=7), Cx50 KO (n=7), MIP KO (n=7) and dKO (n=7) lenses at P15. ***, $P < 0.001$; ****, $P < 0.0001$.

Fig. S1

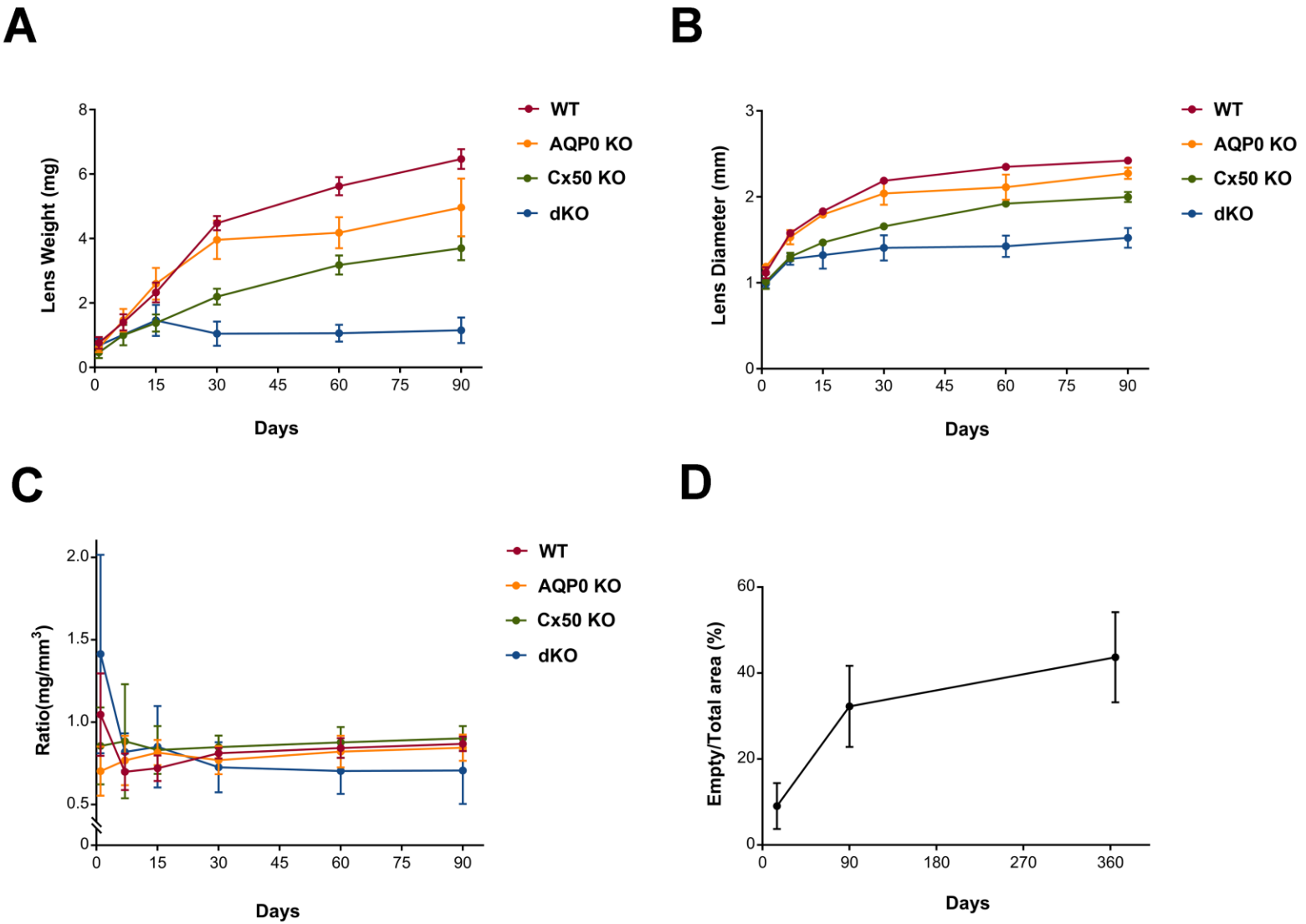
A
Lens Weight (mg)
Days
WT
AQP0 KO
Cx50 KO
dKO
B
Lens Diameter (mm)
Days
WT
AQP0 KO
Cx50 KO
dKO
C
Ratio(mg/mm3)
Days
WT
AQP0 KO
Cx50 KO
dKO
D
Empty/Total area (%)
Days

Fig. S2

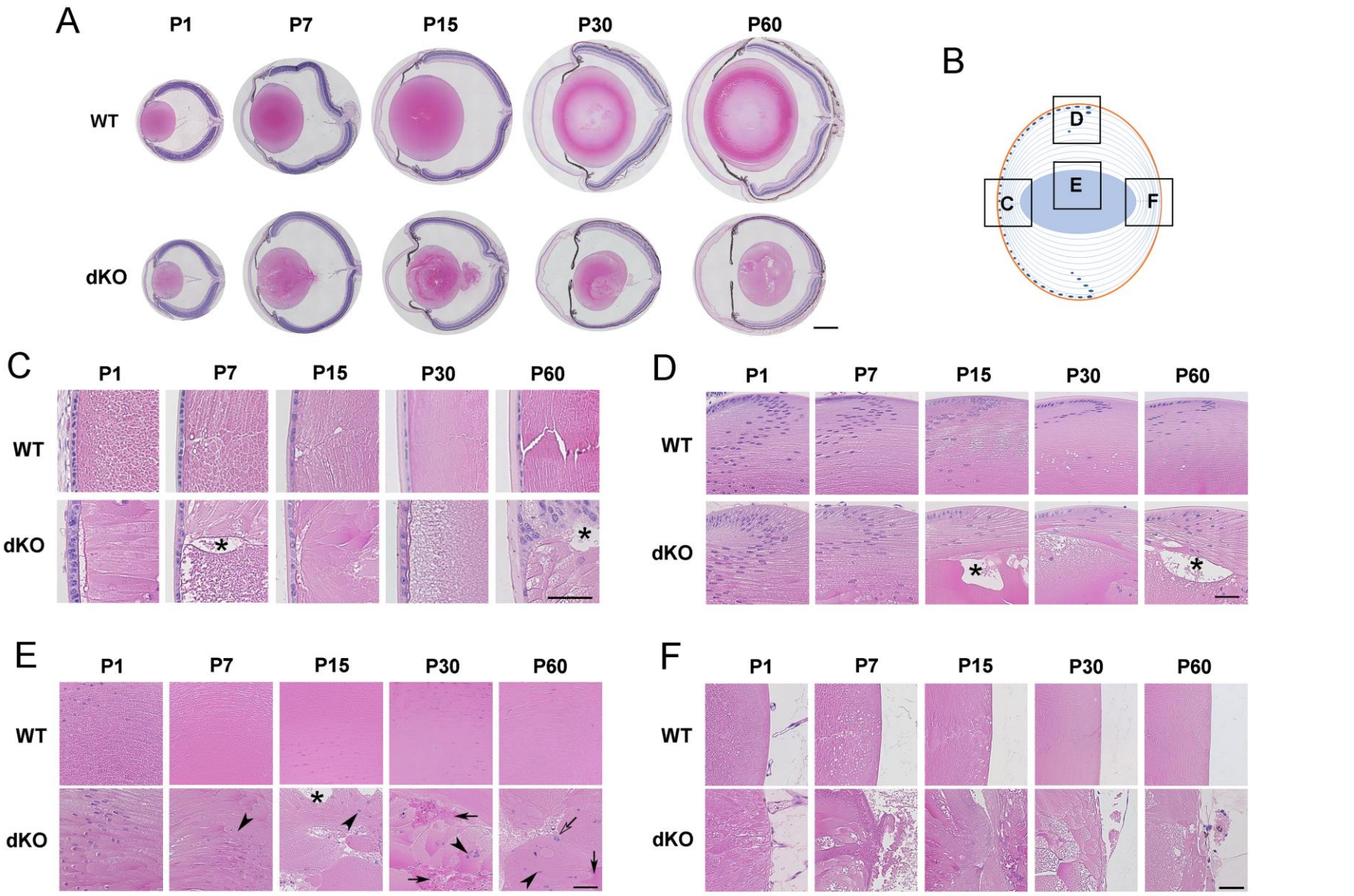
A
P1
P7
P15
P30
P60
WT
dKO
B
D
E
C
F
C
P1
P7
P15
P30
P60
WT
dKO
D
P1
P7
P15
P30
P60
WT
dKO
E
P1
P7
P15
P30
P60
WT
dKO
F
P1
P7
P15
P30
P60
WT
dKO

Fig. S3

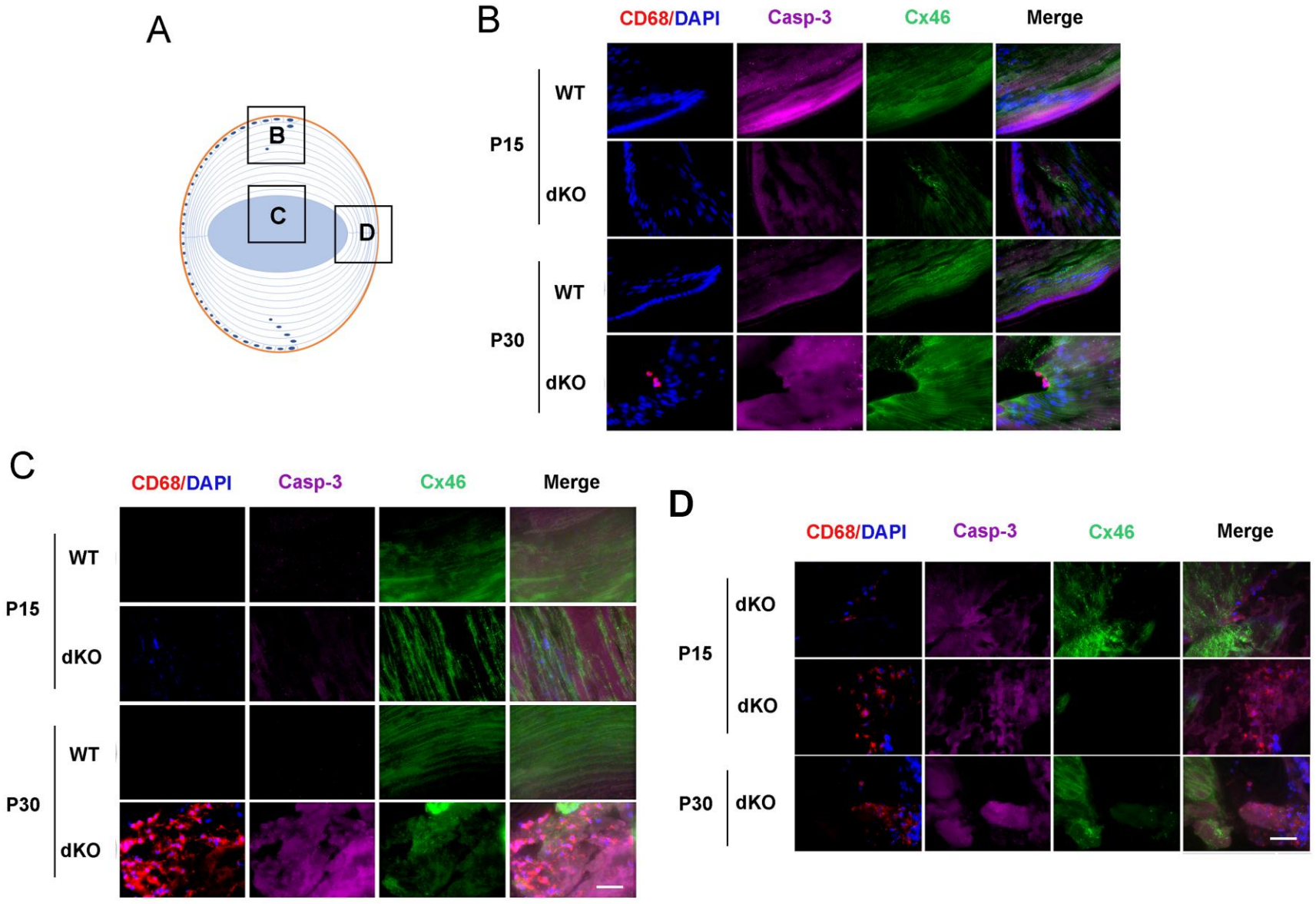
A
B
C
D
B
CD68/DAPI
Casp-3
Cx46
Merge
P15
WT
dKO
P30
WT
dKO
C
CD68/DAPI
Casp-3
Cx46
Merge
P15
WT
dKO
P30
WT
dKO
D
CD68/DAPI
Casp-3
Cx46
Merge
P15
dKO
dKO
P30
dKO

Fig. S4

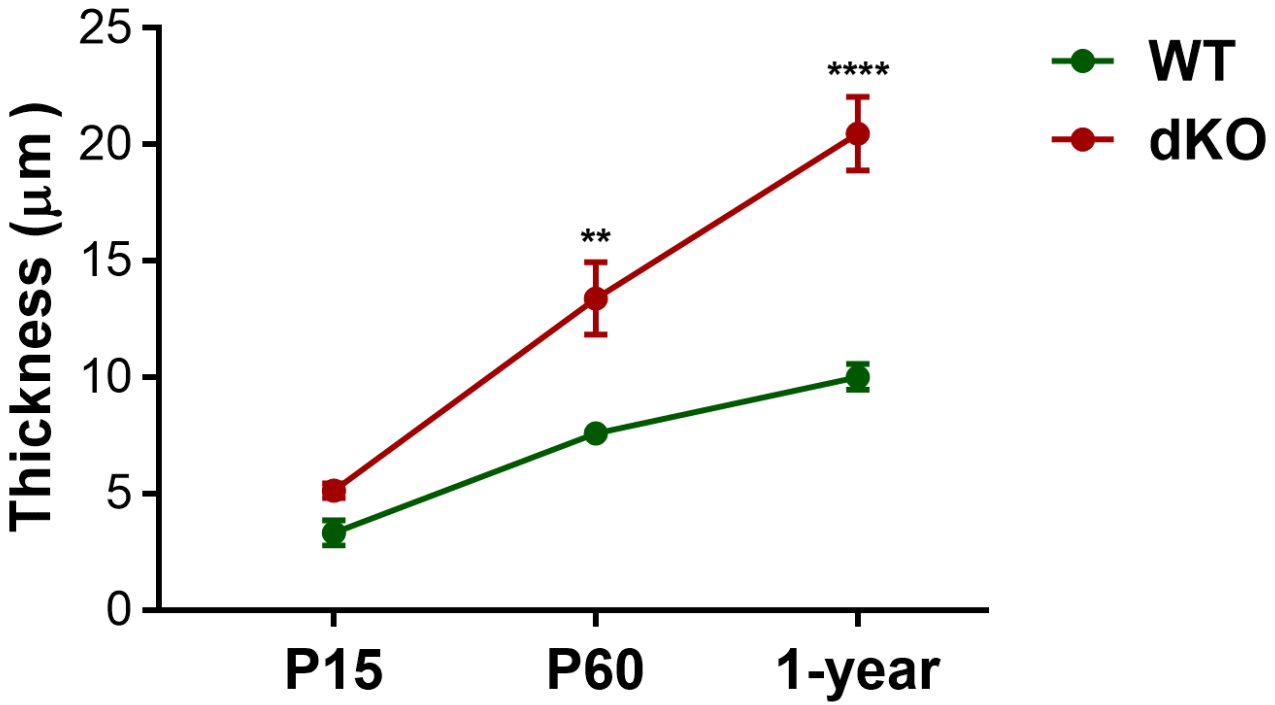

Fig. S5

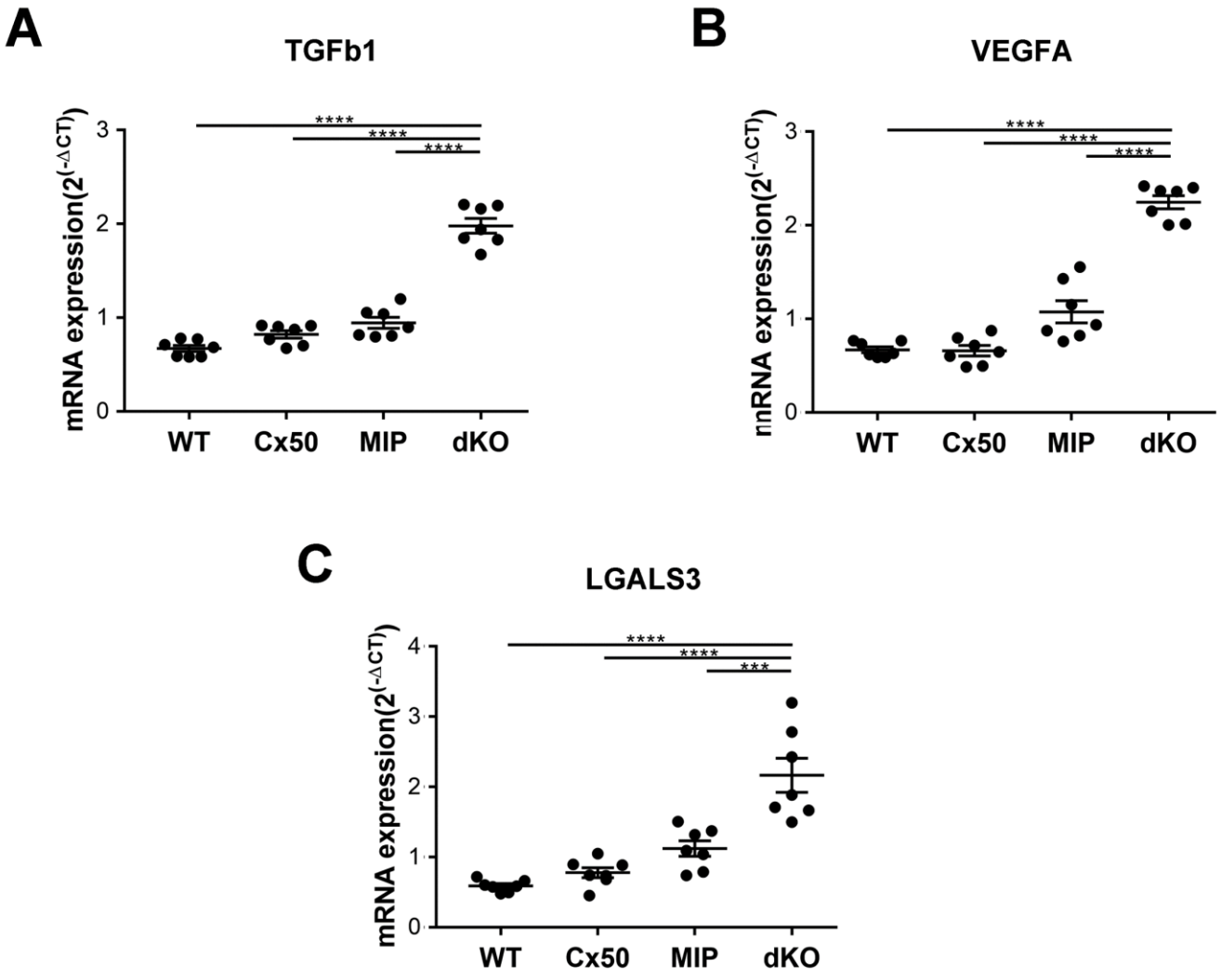
A
TGFb1
mRNA expression(2^(-ΔCT))
0
1
2
3
****
****
****
WT
Cx50
MIP
dKO
B
VEGFA
mRNA expression(2^(-ΔCT))
0
1
2
3
****
****
****
WT
Cx50
MIP
dKO
C
LGALS3
mRNA expression(2^(-ΔCT))
0
1
2
3
4
****
****
***
WT
Cx50
MIP
dKO